

Zonotopic Set-Membership State Estimation for Switched LPV Systems

Shuang Zhang* Vicenc Puig* Sara Ifqir**

* *Institut de Robòtica i Informàtica Industrial (CSIC-UPC), Carrer Llorens Artigas, 4-6, 08028 Barcelona, Spain (e-mail: {shuang.zhang, vicenc.puig}@upc.edu).*

** *CRISTAL, UMR CNRS 9189, Centrale Lille Institut, Cité Scientifique, 59651 Villeneuve d'Ascq, France (e-mail: sara.ifqir@centralelille.fr)*

Abstract: This paper addresses the state estimation problem for switched discrete-time Linear Parameter Varying (LPV) systems with measurable and unmeasurable scheduling parameters. A zonotopic switched polytopic state estimator, considering parameter uncertainty, is proposed based on a Set-Membership Approach (SMA). Taking Average Dwell Time (ADT) into account, a new criterion is proposed to guarantee the convergence of the estimation. An application to vehicle lateral dynamics state estimation is used as case study. Simulation results reveal the effectiveness of the proposed algorithm and demonstrate advantages over the existing methods.

Copyright © 2023 The Authors. This is an open access article under the CC BY-NC-ND license (<https://creativecommons.org/licenses/by-nc-nd/4.0/>)

Keywords: Set-membership estimation, state estimation, switched polytopic LPV system, parameter uncertainty, average dwell time, zonotopes

1. INTRODUCTION

Switched systems are an important class of hybrid dynamic systems, consisting of a series of subsystems and a switching discrete law. In recent years, switched systems have been widely investigated due to their ability to represent complex and nonlinear behaviours. Particularly, when a system operates in a wide operating range and parameter variations, a design of switched estimators/controllers could provide a less conservative performance compared to a single estimator/controller. As state estimation plays an important role in state feedback control and fault diagnosis, it attracted considerable attention in the switched system field during the last decades (Alessandri and Colletta, 2001; Ethabet et al., 2018; Zammali et al., 2020).

Moreover, there exist great challenges in practical applications when the state estimation encounters modelling uncertainties, such as: unknown parameters, process disturbances or measurement noises. Hence, the observer design needs to be robust against these uncertainties. In this regard, considerable results about robust H_∞ filter can be found for switched systems (Zhang et al., 2007; Belkhiat et al., 2011). An alternative is to consider the bounded-error description (Puig et al., 2003; Alamo et al., 2005), where the modelling uncertainties are assumed to be unknown but bounded by priori known bounds. In this context, the set-membership estimator has been employed, where the uncertainties are described using several types of sets, such as intervals, ellipsoids, and zonotopes. Considering that the zonotopic implementation can effectively

eliminate wrapping effects, the zonotopic set-membership approach can obtain more accurate results (Combastel, 2003). Therefore, it has been widely applied to state estimation, and fault detection (Puig, 2010; Le et al., 2013; Tang et al., 2020).

Regarding the recent studies on zonotopic set-membership estimation for switched systems, Fei et al. (2021) proposed a zonotopic state estimator for switched systems. A switched P-radius and L_∞ performance index are adopted to guarantee the convergence and boundness of the zonotopic intersection. However, the proposed ADT-based constraints lead to conservative estimation results. Ifqir et al. (2022) proposed a new P-radius based criterion to reduce the size of the zonotopic intersection at each sample time. The authors presented a less complex solution with less conservative performance. However, this work did not consider the ADT when designing the switched estimator.

This paper proposes a zonotopic SMA-based state estimator for discrete-time switched LPV systems affected by parametric uncertainties, bounded disturbance and noises. The estimator correction matrix design is formulated as an optimization problem in terms of Linear Matrix Inequalities (LMIs) using a less conservative P-radius minimization criterion and ADT constraint. The objective is to find admissible switching signals such that the designed estimator is convergent and stable. The main contributions of this paper are as follows: 1) This paper proposes a new approach for set-membership state estimation of switched LPV systems subject to parametric uncertainties, bounded disturbance and noises. 2) Compared with Fei et al. (2021), a less conservative P-radius based criterion with ADT is proposed for the convergence and stability of the switched LPV state estimator.

* This work has been co-financed by the Spanish State Research Agency (AEI) and the European Regional Development Fund (ERFD) through the project SaCoAV (ref. MINECO PID2020-114244RB-I00).

The rest of the paper is structured as follows: In Section 2, system description and bounded parametric uncertainty are presented. In Section 3, a zonotopic set-membership state estimation approach for switched discrete-time LPV system is proposed. First, the switched LPV state estimator is implemented using zonotopes. Then, a set of LMI constraints is proposed to minimize the size of the zonotopic intersection and guarantee the stability of the switched estimator. Section 4 illustrates the effectiveness of the proposed approach through an application to vehicle lateral dynamics state estimation. Finally, Section 5 draws general conclusions and possible future work.

Notations: In the following, \mathbb{R}^n denotes the set of n -dimensional real numbers and \oplus denotes the Minkowski sum. The matrices are written using capital letter, e.g., A , the calligraphic notation is used for denoting sets, e.g., \mathcal{X} , the interval matrices are denoted by capital letter with square brackets, e.r., $[A]$, $[\underline{x}, \bar{x}]$ is an interval with lower bound \underline{x} and upper bound \bar{x} . Given a box $M = ([a_1, b_1], \dots, [a_n, b_n])^T$, $\text{mid}(M)$ denotes its center and $\text{diam}(M) = (b_1 - a_1, \dots, b_n - a_n)^T$. $\text{rs}(H)$ is a diagonal matrix such that $\text{rs}(H)_{ii} = \sum_{j=1}^m |H_{ij}|, i = 1, \dots, n$. For simplification, the time instant $k + 1, k - 1$ is presented by $+, -,$ respectively, e.g., $x(k + 1) = x(+)$.

Preliminaries:

Lemma 1. Zonotope inclusion (Alamo et al., 2005): Consider a family of zonotopes represented by $Z = p \oplus [M]\mathbf{B}^m$ where $p \in \mathbb{R}^n$ is a real vector and $[M] \in \mathbb{R}^{n \times m}$ is an interval matrix. A zonotope inclusion, denoted by $\diamond(Z)$, is defined by

$$\diamond(Z) = p \oplus [\text{mid}([M]) \quad \text{rs}(\text{diam}([M])/2)] \begin{bmatrix} \mathbf{B}^m \\ \mathbf{B}^n \end{bmatrix}$$

where $\text{rs}(\text{diam}([M])/2)$ represents the row sum diagonal matrix of $\text{diam}([M])/2$. Under the definitions, $Z \subseteq \diamond(Z)$.

Lemma 2. State zonotope inclusion (Guerra et al., 2008): Given $\mathcal{X}_{k+1} = [A]\mathcal{X}_k \oplus [B]u_k$, where $[A]$ and $[B]$ are interval matrices and u_k is the input at time instant k , considering \mathcal{X}_k as a zonotope with the center $c_{x,k}$ and the shape matrix $R_{x,k}$ such $\mathcal{X}_k = \langle c_{x,k}, R_{x,k} \rangle$, the zonotopic state at the next time instant $k+1$ defined as \mathcal{X}_{k+1} is bounded by a zonotope $\mathcal{X}_{k+1}^e = \langle c_{x,k+1}, R_{x,k+1} \rangle$, with

$$\begin{aligned} c_{x,k+1} &= \text{mid}([A])c_{x,k} + \text{mid}([B])u_k, \\ R_{x,k+1} &= \left[\text{seg}(\diamond([A]R_{x,k})) \quad \frac{\text{diam}([A])}{2}c_{x,k} \quad \frac{\text{diam}([B])}{2}u_k \right] \end{aligned}$$

where $\text{seg}(\diamond([A]R_{x,k}))$ means computing the zonotope segment matrix with Lemma 1.

Property 3. Zonotope intersection (Alamo et al. (2005)): Given the zonotope $\mathcal{Z} = \langle c_z, R_z \rangle \in \mathbb{R}^n$, the strip $\mathcal{S} = \{x \in \mathbb{R}^n : |Cx - d| \leq \sigma\}$ and the vector $\lambda \in \mathbb{R}^n$, the intersection between the zonotope and the strip is defined as $\mathcal{Z} \cap \mathcal{S} = \langle c, R \rangle$, where $c = c_z + \lambda(d - Cc_z)$ and $R(\lambda) = [(I - \lambda C)R_z \quad \sigma\lambda]$.

2. SYSTEM DESCRIPTION

Consider the following switched discrete-time LPV system subject to parameter uncertainties, disturbance and measurement noises:

$$\begin{cases} x(+) = A_{\sigma(k)}(\rho(k), \xi(k))x(k) + B_{\sigma(k)}(\rho(k), \xi(k))u(k) + Ew(k) \\ y(k) = Cx(k) + Fv(k) \end{cases} \quad (1)$$

where $x(k) \in \mathbb{R}^{n_x}$ is the state, $u(k) \in \mathbb{R}^{n_u}$ is the control input, $y(k) \in \mathbb{R}^{n_y}$ is the measured output. $w(k) \in \mathbb{R}^{n_w}$ and $v(k) \in \mathbb{R}^{n_v}$ are the process and measurement noises, respectively, assumed to be unknown but bounded. $\sigma(k) : \mathbb{R}^+ \rightarrow \mathcal{I} = \{1, 2, \dots, I\}$ is a known switching signal assumed to be on-line available. The sequence $k_1, k_2 \dots k_l, k_{l+1}, \dots, k_{N_{\sigma}(k_0, K)}$ represents the switching instants on the interval $[k_0, K]$, where $k_0 = 0$ denotes the initial time, k_l denotes the l^{th} switching instant and the active i^{th} subsystem ($\sigma(k) = i$) when $k \in [k_l, k_{l+1})$. And σ satisfies the ADT switching scheme (Liberzon, 2003). $A(\rho(k), \xi(k)) \in \mathbb{R}^{n_x \times n_x}$ and $B(\rho(k), \xi(k)) \in \mathbb{R}^{n_x \times n_u}$ are unknown parametric matrices depending respectively on the measurable and unmeasurable scheduling vectors $\rho(k) \in \mathbb{R}^{n_r}$ and $\xi(k) \in \mathbb{R}^{n_s}$. $E \in \mathbb{R}^{n_x \times n_w}$, $F \in \mathbb{R}^{n_y \times n_v}$ and $C \in \mathbb{R}^{n_y \times n_x}$ are constant matrices. Moreover, the additive uncertainties are assumed to be bounded by a unit hypercube expressed as the centered zonotopes, i.e., $w_k \in \mathcal{W} = \langle 0, I_{n_w} \rangle$, $v_k \in \mathcal{V} = \langle 0, I_{n_v} \rangle$, where $I_{n_w} \in \mathbb{R}^{n_w \times n_w}$ and $I_{n_v} \in \mathbb{R}^{n_v \times n_v}$ denotes the identity matrices. It is assumed that the unknown scheduling vector $\xi(k)$ is composed by a priori known constant nominal value ξ_0 which is affected by an unknown constant uncertainty $\Delta\xi(k)$ such that $\xi(k) = \xi_0 + \Delta\xi(k)$. Therefore, the state matrices can be written as a nominal part plus an uncertain part as:

$$\begin{aligned} A_{\sigma(k)}(\rho(k), \xi(k)) &= A_{\sigma(k)}(\rho(k), \xi_0) + \Delta A_{\sigma(k)}(\rho(k), \Delta\xi(k)) \\ B_{\sigma(k)}(\rho(k), \xi(k)) &= B_{\sigma(k)}(\rho(k), \xi_0) + \Delta B_{\sigma(k)}(\rho(k), \Delta\xi(k)) \end{aligned} \quad (2)$$

For simplification, we denote the nominal part $A_{\sigma(k)}(\rho(k), \xi_0)$ and $B_{\sigma(k)}(\rho(k), \xi_0)$ by $A_{\sigma(k)}(\rho(k))$, $B_{\sigma(k)}(\rho(k))$, respectively.

2.1 Switched LPV system

According to Chen and Patton (2012), the uncertainties on system matrices caused by the uncertain parameter $\xi(k)$ can be approximated by an uncertain term. In this regard, the system (1) can be rewritten as:

$$\begin{cases} x(+) = A_{\sigma(k)}(\rho(k))x(k) + B_{\sigma(k)}(\rho(k))u(k) \\ \quad + D_{\sigma(k)}(\rho(k))d(k) + Ew(k) \\ y(k) = Cx(k) + Fv(k) \end{cases} \quad (3)$$

with

$$\begin{aligned} \Delta A_{\sigma(k)}(\rho(k), \Delta\xi(k))x(k) + \Delta B_{\sigma(k)}(\rho(k), \Delta\xi(k))u(k) \\ \approx D_{\sigma(k)}(\rho(k))d(k), d(k) \in [-1, 1]^{n_d} = \langle 0, I_{n_d} \rangle \end{aligned}$$

where $d(k)$ is a disturbance, namely, an unknown but constant vector. Moreover, $D_{\sigma(k)}(\rho(k))$ is the associated non-empty distribution matrix of suitable dimensions that shows the direction of the parametric uncertainty.

Furthermore, considering that variable $\rho(k)$ is on-line measurable and setting it as the scheduling variable lead to the following switched polytopic form of system (3):

$$\begin{cases} x(+) = \sum_{j=1}^N h_{\sigma(k)}^j(\rho(k)) (A_{\sigma(k)}^j x(k) + B_{\sigma(k)}^j u(k) \\ \quad + D_{\sigma(k)}^j d(k)) + Ew(k) \\ y(k) = Cx(k) + Fv(k) \end{cases} \quad (4)$$

with $\Delta A_{\sigma(k)}^j(\Delta\xi)x(k) + \Delta B_{\sigma(k)}^j(\Delta\xi)u(k) \approx D_{\sigma(k)}^j d(k)$, N is the number of the submodels, $h_{\sigma(k)}^j(\rho(k))$ is the weighting function for the j^{th} sub-model, which is dependent on the parameter $\rho(k)$ and fulfilled by the following properties

$$\sum_{j=1}^N h_{\sigma(k)}^j(\rho(k)) = 1, \quad 0 \leq h_{\sigma(k)}^j(\rho(k)) \leq 1, \quad \forall j \in \mathcal{J} = \{1, \dots, N\}$$

In order to obtain the bound of the uncertainty term $\Delta A_i^j(\Delta\xi)x(k) + \Delta B_i^j(\Delta\xi)u(k)$, $\forall i \in \mathcal{I}, j \in \mathcal{J}$ with zonotopes, it is assumed that the system states and inputs belong to the interval vectors $[X] = [\underline{x}, \bar{x}]$ and $[U] = [\underline{u}, \bar{u}]$, respectively, which can be represented by the following zonotopic sets:

$$x(k) \in \mathcal{X} = \langle p_x, H_x \rangle, p_x = \text{mid}([X]), H_x = \text{rs}\left(\frac{\text{diam}([X])}{2}\right)$$

$$u(k) \in \mathcal{U} = \langle p_u, H_u \rangle, p_u = \text{mid}([U]), H_u = \text{rs}\left(\frac{\text{diam}([U])}{2}\right)$$

Due to the parametric uncertainty, the system matrices are bounded by the interval matrices: $\Delta A_i^j(\Delta\xi) \in [\Delta A_i^j]$, $\Delta B_i^j(\Delta\xi) \in [\Delta B_i^j]$. Then, it follows

$$\Delta A_i^j(\Delta\xi)x(k) + \Delta B_i^j(\Delta\xi)u(k) \in [\Delta A_i^j]\mathcal{X} \oplus [\Delta B_i^j]\mathcal{U}.$$

Considering Lemma 2, we have,

$$[\Delta A_i^j]\mathcal{X} \oplus [\Delta B_i^j]\mathcal{U} = \langle 0, D_i^j \rangle = \langle 0, [S_1 \ S_2 \ S_3 \ S_4] \rangle, \quad (5)$$

where

$$S_1 = \text{seg}(\diamond([\Delta A_i^j]H_x)) = \text{rs}\left(\frac{\text{diam}([\Delta A_i^j])}{2}\right)|H_x|,$$

$$S_2 = \text{seg}(\diamond([\Delta B_i^j]H_u)) = \text{rs}\left(\frac{\text{diam}([\Delta B_i^j])}{2}\right)|H_u|,$$

$$S_3 = \frac{\text{diam}([\Delta A_i^j])}{2}p_x, S_4 = \frac{\text{diam}([\Delta B_i^j])}{2}p_u.$$

Remark 4. It is worth noting that the intervals $[X]$ and $[U]$ may correspond to the theoretical maximum bounds or physical limits in the case of real applications.

So far, a switched polytopic LPV model with parametric uncertainties is built. A set-membership state estimator for this model will be designed in the next section.

3. SET-MEMBERSHIP ZONOTOPIC SWITCHED LPV STATE ESTIMATOR

In this section, a set-membership state estimation approach for the switched polytopic LPV system (4) is proposed. This approach is based on the parameterized zonotope intersection, which can be implemented by the following Algorithm 1.

Algorithm 1: SMA-based State Estimation.

1. Prediction Step Given the switched polytopic LPV system (4), compute the zonotopic uncertain state set

$$\bar{\mathcal{X}}_k = \sum_{j=1}^N h_{\sigma(k)}^j(\rho(-)) \left(A_{\sigma(k)}^j \hat{\mathcal{X}}_- \oplus B_{\sigma(k)}^j u_- \oplus D_{\sigma(k)}^j \right) \oplus EW.$$

2. Measurement Step Compute the measurement state set \mathcal{X}_{y_k} by using the measurements y_k .

3. Correction Step Compute the outer approximation $\hat{\mathcal{X}}_k$ of $\bar{\mathcal{X}}_k \cap \mathcal{X}_{y_k}$.

3.1 Zonotopic Implementation for Set-membership State Estimation

For implementing the set-membership state estimation approach with zonotopes, the following theorem is proposed.

Theorem 5. Consider the switched polytopic LPV system (4), let $\hat{\mathcal{X}}_k = \langle c_k, R_k \rangle \in \mathbb{R}^{n_x}$ be the zonotopic estimated state, where $c_k \in \mathbb{R}^{n_x}$ and $R_k \in \mathbb{R}^{n_x \times n_r}$ represent the center and

shape matrix, respectively. Assume that the initial state \hat{x}_0 belongs to the set $\hat{\mathcal{X}}_0 = \langle c_0, R_0 \rangle$, the estimated state can be propagated as follows:

$$c_k = \bar{c}_k + \sum_{j=1}^N h_{\sigma(-)}^j(\rho-) \lambda_{\sigma(-)}^j (y_k - C\bar{c}_k) \quad (7a)$$

$$R_k = \sum_{i=1}^N h_{\sigma(-)}^j(\rho-) \left[\left(I_{n_x} - \lambda_{\sigma(k)}^j C \right) \bar{R}_k \lambda_{\sigma(-)}^j F \right] \quad (7b)$$

with

$$\bar{c}_k = \sum_{j=1}^N h_{\sigma(-)}^j(\rho-) \left(A_{\sigma(-)}^j c_- + B_{\sigma(-)}^j u_- \right) \quad (8a)$$

$$\bar{R}_k = \sum_{j=1}^N h_{\sigma(-)}^j(\rho-) \left[A_{\sigma(-)}^j \hat{R}_- \quad D_{\sigma(-)}^j \quad E \right] \quad (8b)$$

where $\langle \bar{c}_k, \bar{R}_k \rangle$ denotes the zonotopic predicted states.

Proof. Considering the switched system (3) with the inclusion $x_- \in \hat{\mathcal{X}}_- = \langle c_-, R_- \rangle$, the zonotopic predicted state set can be computed as:

$$\begin{aligned} \bar{\mathcal{X}}_k = \langle \bar{c}_k, \bar{R}_k \rangle = & A_{\sigma(-)}(\rho(-)) \langle c_-, R_- \rangle \oplus \langle 0, D_{\sigma(-)}(\rho(-)) \rangle \\ & \oplus \langle B_{\sigma(-)}(\rho(-)) u(k), 0 \rangle \oplus \langle 0, E \rangle \end{aligned} \quad (9)$$

Considering the polytopic form, \bar{c}_k and \bar{R}_k can be derived. In addition, the measurement state set \mathcal{X}_{y_k} is computed by considering current measurement y_k as

$$\mathcal{X}_{y_k} = \{x \in \mathbb{R}^{n_x} : y_k - Cx \in F \langle 0, I_{n_y} \rangle\} \quad (10)$$

Thus, the estimated state $\hat{\mathcal{X}}_k$ can be obtained through an outer approximation of the intersection between the zonotope (9) and the measurement state set (10). Based on Property 3, for any switched correction matrix $\lambda_{\sigma(k)}(\rho(-)) \in \mathbb{R}^{n_x \times n_y}$, the intersection is obtained as:

$$\begin{aligned} \hat{\mathcal{X}}_k = \langle c_k, R_k \rangle = & \langle \bar{c}_k + \lambda_{\sigma(k)}(\rho(-))(y_k - C\bar{c}_k), \\ & [(I_{n_x} - \lambda_{\sigma(k)}(\rho(-))C)\bar{R}_k \quad \lambda_{\sigma(k)}(\rho(-))F] \rangle \end{aligned} \quad (11)$$

Therefore, the estimated state is derived as in (7) after applying the polytopic form of the correction matrix $\lambda_{\sigma(-)}(\rho(-)) = \sum_{j=1}^N h_{\sigma(-)}^j(\rho(-)) \lambda_{\sigma(-)}^j$.

3.2 Optimal Switched Polytopic Correction Matrix Design

This design consists in computing a weighting matrix $P_i = P_i^T \in \mathbb{R}^{n_x \times n_x} \geq 0$ and a parameter-dependent correction matrix $\lambda_i(\rho(k))$ to guarantee that the size of the zonotopic state estimation set $\hat{\mathcal{X}}_k$ is decreased, $\forall i \in \mathcal{I}, \forall k \geq 0$. To reduce the conservatism, the size of $\hat{\mathcal{X}}_k$ is measured by mode-dependent P_i -radius as follows:

$$\begin{aligned} l_{\sigma(-)}(k) &= \max_{x(k) \in \hat{\mathcal{X}}_k} \|x(k) - c_k(\lambda_{\sigma(-)}(\rho(-)))\|_{P_{\sigma(-)}}^2 \\ &= \max_{z \in \mathbb{B}^{n_r}} \|R_k(\lambda_{\sigma(-)}(\rho(-)))z\|_{P_{\sigma(-)}}^2 \end{aligned} \quad (12)$$

where $P_{\sigma(-)} = P_i, \forall i \in \mathcal{I}$ is the weighting matrix for the i -th subsystem.

Definition 6. For a switching signal $\sigma(k)$ and any $K > k > 0$, let $N_{\sigma}(k, K)$ denote the switching times of σ during the interval $[k, K]$. If for any given $N_0 > 0$ and $\tau_a > 0$, we have

$$N_{\sigma}(k, K) \leq N_0 + \frac{K - k}{\tau_a}, \quad \forall K \geq k > 0,$$

then N_0 and τ_a are called the chatter bound and ADT respectively (Hespanha and Morse, 1999). We can set $N_0 = 0$ as commonly used in the literature.

In the following, the conditions will be proposed to minimize the effects of uncertainties and guarantee that the size of $\hat{\mathcal{X}}_k$ is convergent with ADT switching.

Lemma 7. Consider the switched system (3), if there exist scalars $\varepsilon_{\sigma(k)} \in (0, 1)$ and $\gamma_{\sigma(k)}$ associated with each subsystem $\sigma(k) = i$, constants $\gamma_i, \alpha_2 > \alpha_1 > 0$ such that

$$\forall \sigma(k) = i \in \mathcal{I}, \alpha_1 \Omega_i(k+1) \leq l_i(k) \leq \alpha_2 \Omega_i(k+1), \quad (13)$$

$$l_i(k+1) \leq \varepsilon_i l_i(k) + \gamma_i \delta_i \quad (14)$$

where $\Omega_i(k+1) = \max_{x(+)\in\hat{\mathcal{X}}_+} \|x(+)-c_+(\lambda_i(\rho(k)))\|$, $\alpha_1 = \max \text{eig}(P_i)$, $\alpha_2 = \max \text{eig}(P_i)$, δ_i is a positive switched constant that represents the maximum influence of process disturbance, parametric uncertainty and measurement noises as follows:

$$\delta_i = \max_{s_1 \in \mathbf{B}^{n_d}} \|D_i(\rho(k))s_1\|_2^2 + \max_{s_2 \in \mathbf{B}^{n_x}} \|Es_2\|_2^2 + \max_{s_3 \in \mathbf{B}^{n_y}} \|Fs_3\|_2^2$$

Then the size of the zonotopic intersection $\hat{\mathcal{X}}_k$ is bounded and decreased for any switching signal with ADT

$$\tau_a > \tau_a^* = -\ln \mu / \ln(\varepsilon_i), \mu = \alpha_2 / \alpha_1. \quad (15)$$

Proof. Considering the inequality (14), we have

$$l_i(k+1) \leq \varepsilon_i l_i(k) \leq \varepsilon_i l_i(k) + \gamma_i \delta_i \quad (16)$$

$\forall k-1 \in [k_l, k_{l+1})$, the i^{th} subsystem is active, for all $i, q \in \mathcal{I} \times \mathcal{I}, i \neq q$, it leads to

$$l_i(k-1) \leq \varepsilon_i^{k-k_l-1} l_i(k_l) \leq \varepsilon_i^{k-k_l-1} \frac{l_i(k_l)}{l_q(k_l)} l_q(k_l), \quad (17)$$

where

$$l_i(k_l) = \max_{x_{k_l} \in \hat{\mathcal{X}}_{k_l}} \|x_{k_l} - c_{k_l}(\lambda_i(\rho(k_l-1)))\|_{P_i}^2, \quad (18)$$

$$l_q(k_l) = \max_{x_{k_l} \in \hat{\mathcal{X}}_{k_l}} \|x_{k_l} - c_{k_l}(\lambda_q(\rho(k_l-1)))\|_{P_q}^2. \quad (19)$$

Since $\alpha_1 I_{n_x} \leq P_i \leq \alpha_2 I_{n_x}$, $\alpha_1 I_{n_x} \leq P_q \leq \alpha_2 I_{n_x}$, using condition (13), we have

$$\alpha_1 \Omega_i(k_l) \leq l_i(k_l) \leq \alpha_2 \Omega_i(k_l) \quad (20)$$

$$\alpha_1 \Omega_q(k_l) \leq l_q(k_l) \leq \alpha_2 \Omega_q(k_l) \quad (21)$$

with $\Omega_i(k_l) = \max_{x_{k_l} \in \hat{\mathcal{X}}_{k_l}} \|x_{k_l} - c_{k_l}(\lambda_i(\rho(k_l-1)))\|$, and $\Omega_q(k_l) = \max_{x_{k_l} \in \hat{\mathcal{X}}_{k_l}} \|x_{k_l} - c_{k_l}(\lambda_q(\rho(k_l-1)))\|$.

As $c_{k_l}(\lambda_i(\rho(k_l-1))) \neq c_{k_l}(\lambda_q(\rho(k_l-1)))$, then $\Omega_i(k_l) < \Omega_q(k_l)$. Thus, inequality (17) becomes

$$l_i(k-1) \leq \varepsilon_i^{k-k_l-1} \frac{\alpha_2 \Omega_i(k_l)}{\alpha_1 \Omega_q(k_l)} l_q(k_l) \leq \varepsilon_i^{k-k_l-1} \frac{\alpha_2}{\alpha_1} l_q(k_l)$$

At the switching time instant $k-1 = k_l$, it has

$$l_i(k_l) \leq \mu l_q(k_l) \quad (22)$$

where $\mu = \frac{\alpha_2}{\alpha_1} > 1$. Therefore, the size of the zonotopic intersection is decreasing for each subsystem, and bounded when the subsystem switches, which ends the proof.

If (14) holds, then when $k \rightarrow \infty, \forall i \in \mathcal{I}, l_\infty = \varepsilon_i l_\infty + \gamma_i \delta_i$, it follows that $l_\infty = \gamma_i \frac{\delta_i}{1-\varepsilon_i}$, which shows the equality of minimizing the P_i -radius (12), for given ε_i and δ_i , and minimizing the attenuation gain γ_i . Then, the computation of the parameter-dependent correction matrix $\lambda_i(\rho(k))$ for each subsystem is transformed into solving a Multi-Objective Global Minimum Optimization problem with LMIs constraints according to the following theorem.

Theorem 8. Inequality (13) and (14) hold, $\forall i \in \mathcal{I}, j \in \mathcal{N}$, if there exists a matrix $W_i^j \in \mathbb{R}^{n_x \times n_y}$, a positive definite matrix $P_i^j \in \mathbb{R}^{n_x \times n_x}$, scalars $\gamma > 0, \gamma_i^j > 0$ for given scalar

$\varepsilon_i \in (0, 1)$ that are obtained by solving the following LMI optimization problem

$$\begin{aligned} \min_{W_i^j, P_i^j, \gamma_i} \quad & \gamma \\ \gamma_i^j \leq \quad & \gamma \end{aligned} \quad (23a)$$

$$\alpha < P_i^j < \beta \quad (23b)$$

$$\begin{bmatrix} \varepsilon_i P_i^j & 0 & 0 & 0 & A_i^j T (P_i^j - C^T W_i^j T) \\ * & \gamma_i^j D_i^T D_i & 0 & 0 & D_i^j T (P_i^j - C^T W_i^j T) \\ * & * & \gamma_i^j E^T E & 0 & E^T (P_i^j - C^T W_i^j T) \\ * & * & * & \gamma_i^j F^T F & F^T W_i^j T \\ * & * & * & * & P_i^j \end{bmatrix} \geq 0 \quad (23c)$$

where $W_i^j = P_i^j \lambda_i^j, \lambda_i^j = P_i^{j-1} W_i^j$.

Proof. For all $\sigma(k) = i \in \mathcal{I}$, with denoting $\hat{z} = [z^T \ s^T]^T, s = [s_1^T \ s_2^T \ s_3^T]^T$, where $z \in \mathbf{B}^{n_r}, s_1 \in \mathbf{B}^{n_d}, s_2 \in \mathbf{B}^{n_x}, s_3 \in \mathbf{B}^{n_y}$, (14) can be rewritten as

$$\begin{aligned} \max_{\hat{z} \in \mathbf{B}^{n_r+n_d+n_x+n_y}} \quad & \|R_+(\lambda_i(\rho(k)))\hat{z}\|_{P_i}^2 \\ \leq \varepsilon_i \max_{z \in \mathbf{B}^{n_r}} \quad & \|R_k(\lambda_i(\rho(-)))z\|_{P_i}^2 + \gamma_i (\max_{s_1 \in \mathbf{B}^{n_d}} \|D_i(\rho(-))s_1\|_2^2 \\ & + \max_{s_2 \in \mathbf{B}^{n_x}} \|Es_2\|_2^2 + \max_{s_3 \in \mathbf{B}^{n_y}} \|Fs_3\|_2^2) \end{aligned}$$

It follows that

$$\begin{aligned} \max_{\hat{z} \in \mathbf{B}^{n_r+n_d+n_x+n_y}} \quad & (\|R_+(\lambda_i(\rho(k)))\hat{z}\|_{P_i}^2 - \varepsilon_i \|R_k(\lambda_i(\rho(-)))\hat{z}\|_{P_i}^2 \\ & - \gamma_i (\|D_i(\rho(-))s_1\|_2^2 + \|Es_2\|_2^2 + \|Fs_3\|_2^2)) \leq 0 \end{aligned}$$

which is equivalent to the following inequality:

$$\begin{aligned} \hat{z}^T R_+(\lambda_i(\rho(k)))^T P_i R_+(\lambda_i(\rho(k)))\hat{z} - \gamma_i s^T \Lambda_i s \\ - \varepsilon_i z^T R_k(\lambda_i(\rho(-)))^T P_i R_k(\lambda_i(\rho(-)))z \leq 0 \end{aligned} \quad (24)$$

where

$$\Lambda_i = \text{diag}([D_i(\rho(-))^T D_i(\rho(-)) \ E^T E \ F^T F])$$

Recalling that

$$\begin{aligned} R_+(\lambda_i(\rho(k)))\hat{z} = (I - \lambda_i(\rho(k))C)A_i(\rho(k))R_k(\lambda_i(\rho(k)))z \\ + [(I - \lambda_i(\rho(k))C)D_i(\rho(k)) \ (I - \lambda_i(\rho(k))C)E \ \lambda_i(\rho(k))F]s, \end{aligned} \quad (25)$$

which allows to replace $R_+(\lambda_i(\rho(+)))\hat{z}$ in (24) by (25). Then, the following inequality (26) is derived, where

$$Z_i = [(I - \lambda_i(\rho(k))C)D_i \ (I - \lambda_i(\rho(k))C)E \ \lambda_i(\rho(k))F]$$

Since inequality (26) holds, it is equivalent to that the following inequality (27) holds. It is worth noting that due to the space limitation, inequalities (26) and (27) are presented on the next page. With the application of Schur complement, and considering the polytopic form of $\lambda_i(\rho(k)), A_i(\rho(k))$ and $D_i(\rho(k))$, (27) can be rewritten as the following inequality, which is valid for all vertices $\forall j \in \mathcal{J}$:

$$\begin{bmatrix} \varepsilon_i P_i^j & 0 & 0 & 0 & ((I - \lambda_i^j)C)A_i^j T P_i^j \\ * & \gamma_i^j D_i^j T D_i^j & 0 & 0 & ((I - \lambda_i^j)C)D_i^j T P_i^j \\ * & * & \gamma_i^j E^T E & 0 & ((I - \lambda_i^j)C)E^T P_i^j \\ * & * & * & \gamma_i^j F^T F & (\lambda_i^j F)^T P_i^j \\ * & * & * & * & P_i^j \end{bmatrix} \geq 0$$

It's worth noting that the parameters P_i^j and γ_i^j are used to introduce more degrees of freedom and consequently reduce conservatism. Then, (23c) can be derived by applying $W_i^j = P_i^j \lambda_i^j, \lambda_i^j = P_i^{j-1} W_i^j$. Therefore, by minimizing the gain $\gamma_i^j, \forall i \in \mathcal{I}, j \in \mathcal{J}$, the size of the intersection zonotope $\hat{\mathcal{X}}_k$ is equally minimized. In order to solve this multi-objective optimization problem, one objective scalar γ is minimized while the others are transformed into constraints $\gamma_i \leq \gamma$. Hence, we complete the proof.

$$\begin{bmatrix} R_k(\lambda_i(\rho(k)))z \\ s \end{bmatrix}^T \begin{bmatrix} A_i(\rho(k))^T(I - \lambda_i(\rho(k))C)^T P_i(I - \lambda_i(\rho(k))C)A_i(\rho(k)) - \varepsilon_i P_i & * \\ Z_i P_i(I - \lambda_i(\rho(k))C)A_i(\rho(k)) & Z_i P_i Z_i - \gamma_i \Lambda_i \end{bmatrix} \begin{bmatrix} R_k(\lambda_i(\rho(k)))z \\ s \end{bmatrix} \leq 0 \quad (26)$$

$$\begin{bmatrix} \varepsilon_i P_i & 0 \\ 0 & \gamma_i \Lambda_i \end{bmatrix} - \begin{bmatrix} ((I - \lambda_i(\rho(k))C)A_i(\rho(k)))^T P_i \\ Z_i P_i \end{bmatrix} P_i^{-1} \begin{bmatrix} ((I - \lambda_i(\rho(k))C)A_i(\rho(k)))^T P_i \\ Z_i P_i \end{bmatrix}^T \geq 0 \quad (27)$$

4. CASE STUDY

4.1 Vehicle model description

In this section, a vehicle lateral dynamics nonlinear model is given as the following LPV model(Ifqir et al., 2019):

$$\begin{bmatrix} \dot{\beta} \\ \dot{\psi} \end{bmatrix} = \begin{bmatrix} -\frac{c_f + c_r}{mv_x} & \frac{c_r l_r - c_f l_f}{mv_x^2} - 1 \\ \frac{c_r l_r - c_f l_f}{I_z} & -\frac{c_r l_r^2 + c_f l_f^2}{I_z v_x} \end{bmatrix} \begin{bmatrix} \beta \\ \psi \end{bmatrix} + \begin{bmatrix} \frac{c_f}{mv_x} \\ \frac{c_f l_f}{I_z} \end{bmatrix} \delta_f \quad (28)$$

where β and ψ are vehicle sideslip angle and yaw rate, δ_f is the steering angle, m and I_z are the mass and the yaw moment, v_x is the longitudinal velocity, l_f and l_r are the distances from front and rear axle to the center of gravity, c_f, c_r are the cornering stiffness of front and rear tires. It is worth noting that c_f and c_r are not measurable and vary with the surface friction. Then, readjustment variables Δc_r and Δc_f are taken into account to correct the cornering stiffness errors as: $c_f = c_{f0} + \Delta c_f$ and $c_r = c_{r0} + \Delta c_r$, where c_{f0} and c_{r0} represent known nominal values, and Δc_r and Δc_f are assumed to be unknown but bounded.

Denoting β and ψ as states, δ_f as the input, v_x and c_f, c_r as the measurable and unmeasurable scheduling variables, respectively, (28) can be represented by the following LPV model subject to disturbances w and noises v :

$$\begin{cases} \dot{x}(t) = A(\rho(t), \xi(t))x(t) + B(\rho(t), \xi(t))u(t) + Ew(t) \\ y(t) = Cx(t) + Fv(t) \end{cases} \quad (29)$$

where $\rho(t) = v_x$ and $\xi(t) = [c_r \ c_f]^T$, $y(t)$ is the measurement of yaw rate and $v(t)$ is the corresponding measurement noise with distribution matrix F .

In order to obtain the discrete-time LPV model of system (29), Euler's discretization method, with the sampling time $T=0.04s$, is used. It follows that

$$\begin{cases} x(+)=A(\rho(k), \xi(k))x(k)+B(\rho(k), \xi(k))u(k)+Ew(k) \\ y(k)=Cx(k)+Fv(k) \end{cases} \quad (30)$$

where $A(\rho(k), \xi(k)) = I_{n_x} + TA(\rho(k), \xi(k))$, $B(\rho(k), \xi(k)) = TB(\rho(k), \xi(k))$, the disturbance and noise distribution matrices satisfy $W = \begin{bmatrix} 0.001 & 0 \\ 0 & 0.02 \end{bmatrix}$ and $F = 0.03$.

Dividing the region of parameter $\rho(k)$ into I sub-regions, I subsystems are obtained with a switching law $\sigma(k) : \mathbb{R}^+ \rightarrow \mathcal{I} = \{1, 2, \dots, I\}$. Considering the uncertainties on the parameter $\xi(k)$, the state space matrices can be decoupled as (2). Approximating the parametric uncertainties by an uncertain term $D_{\sigma(k)}(\rho(k))d(k)$ and using the sector nonlinearity approach, a switched polytopic LPV representation with I subsystems and 2 sub-models for each subsystem is derived and given as follows:

$$\begin{cases} x(+)=\sum_{j=1}^2 h_{\sigma(k)}^j(\rho(k))(A_{\sigma(k)}^j x(k)+B_{\sigma(k)}^j u(k) \\ \quad +D_{\sigma(k)}^j d(k))+Ew(k) \\ y(k)=Cx(k)+Fv(k) \end{cases} \quad (31)$$

In this paper, the system states and input belong to the intervals $[X(1)] = [-0.06, 0.06]$, $[X(2)] = [-0.5, 0.4]$ and $[U] = [-0.14, 0.08]$. Thus, $D_{\sigma(k)}^j$ can be computed with (5).

4.2 Experimental validation

This subsection will test the performance of the proposed design using experimental data. The experiments are conducted by a vehicle equipped with several sensors on a track of 3.5 km with various curves. The available measurements are yaw rate ψ , steering angle δ_f , and longitudinal speed v_x , shown in figures 1,2, and 3. It is worth noting that the sideslip angle β is measured by a Correvit sensor, which serves only for validation not for the estimator design. Considering the characteristic of the measured longitudinal velocity v_x in Fig.3, the whole parameter space can be divided into three sub-regions according to the following switching rule:

$$\sigma(k) = \begin{cases} 1 & \text{if } 9m.s^{-1} < v_x \leq 13m.s^{-1} \\ 2 & \text{if } 13m.s^{-1} < v_x \leq 16m.s^{-1} \\ 3 & \text{if } 16m.s^{-1} < v_x \leq 20m.s^{-1} \end{cases} \quad (32)$$

and three local models are obtained with the considered switching law shown in Fig.4.

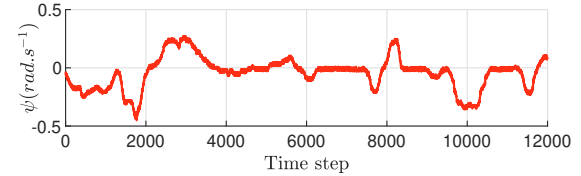


Fig. 1. Yaw rate ψ .

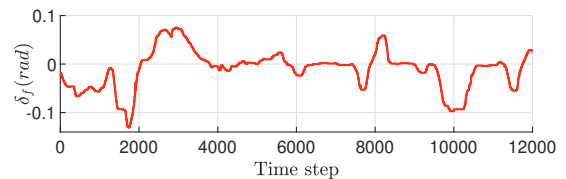


Fig. 2. Steering angle δ_f .

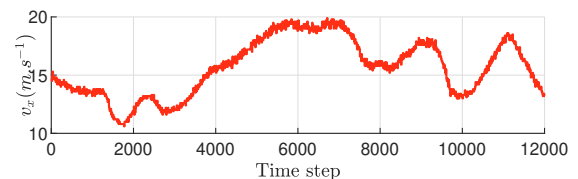


Fig. 3. Longitudinal velocity v_x .

By solving the LMI optimization problem (23) and selecting the scalar $\varepsilon_i = 0.78$, we can obtain the switched polytopic correction matrices $\lambda_{\sigma(k)}^j$ and the corresponding minimum ADT $\tau_a^* = 8.7985$ through (15). Then the actual trajectories of the system states (black line) and the state-bounding intervals (red line) are depicted in Fig.5 and Fig.6. Furthermore, under the same parameters set, a

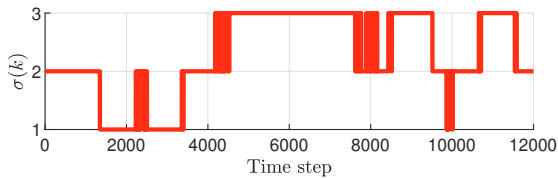


Fig. 4. Switching signal $\sigma(k)$.

comparison is conducted using the SMA-based switched state estimator from subsection A of Fei et al. (2021) for the system (3). As the compared estimation results shown in Fig.5 and Fig.6, it reveals that the proposed method allows to provide a more accurate bounded estimation of the vehicle state variables.

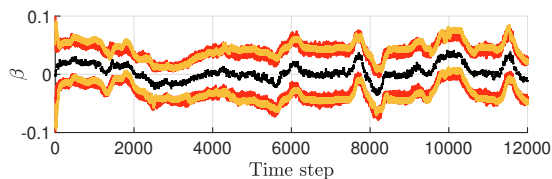


Fig. 5. Set-membership estimation of β using proposed approach (red) and reference approach (orange).

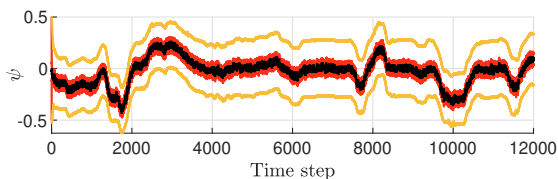


Fig. 6. Set-membership estimation of ψ using proposed approach (red) and reference approach (orange).

5. CONCLUSION

In this paper, a zonotopic switched LPV state estimator using set-membership approach has been proposed for switched discrete-time system with measured and unmeasured parameters. In order to design the switched polytopic correction matrix, the P_i -radius of the intersection zonotope and ADT switching are considered to derive the LMIs conditions. As demonstrated by the application example, this solution is more accurate. As future work, applying the proposed approach to fault diagnosis, such as minimum detectable fault will be investigated.

ACKNOWLEDGEMENTS

This work has been co-financed by the Spanish State Research Agency (AEI) and the European Regional Development Fund (ERFD) through the project SaCoAV (ref. MINECO PID2020-114244RB-I00), by the European Regional Development Fund of the European Union in the framework of the ERDF Operational Program of Catalonia 2014–2020 (ref. 001-P-001643 Looming Factory), by the DGR of Generalitat de Catalunya (SAC group ref. 2017/SGR/482) and by the Chinese Scholarship Council (CSC) under grant (202006120006).

REFERENCES

Alamo, T., Bravo, J.M., and Camacho, E.F. (2005). Guaranteed state estimation by zonotopes. *Automatica*, 41(6), 1035–1043.

- Alessandri, A. and Coletta, P. (2001). Design of luenberger observers for a class of hybrid linear systems. In *International Workshop on Hybrid Systems: Computation and Control*, 7–18. Springer.
- Belkhiat, D., Messai, N., and Manamanni, N. (2011). Design of a robust fault detection based observer for linear switched systems with external disturbances. *Nonlinear Analysis: Hybrid Systems*, 5(2), 206–219.
- Chen, J. and Patton, R.J. (2012). *Robust model-based fault diagnosis for dynamic systems*, volume 3. Springer Science & Business Media.
- Combastel, C. (2003). A state bounding observer based on zonotopes. In *2003 European Control Conference (ECC)*, 2589–2594. IEEE.
- Ethabet, H., Rabehi, D., Efimov, D., and Raïssi, T. (2018). Interval estimation for continuous-time switched linear systems. *Automatica*, 90, 230–238.
- Fei, Z., Yang, L., Sun, X.M., and Ren, S. (2021). Zonotopic set-membership state estimation for switched systems with restricted switching. *IEEE Transactions on Automatic Control*.
- Guerra, P., Puig, V., and Witczak, M. (2008). Robust fault detection with unknown-input interval observers using zonotopes. *IFAC Proceedings Volumes*, 41(2), 5557–5562.
- Hespanha, J.P. and Morse, A.S. (1999). Stability of switched systems with average dwell-time. In *Proceedings of the 38th IEEE conference on decision and control (Cat. No. 99CH36304)*, volume 3, 2655–2660. IEEE.
- Ifqir, S., Dalil, I., Naïma, A.O., and Saïd, M. (2019). Adaptive threshold generation for vehicle fault detection using switched t-s interval observers. *IEEE Transactions on Industrial Electronics*, 67(6), 5030–5040.
- Ifqir, S., Vicenç, P., Dalil, I., Naima, A.O., and Saïd, M. (2022). Zonotopic set-membership state estimation for switched systems. *Journal of the Franklin Institute*.
- Le, V.T.H., Stoica, C., Alamo, T., Camacho, E.F., and Dumur, D. (2013). Zonotope-based set-membership estimation for multi-output uncertain systems. In *2013 IEEE International Symposium on Intelligent Control (ISIC)*, 212–217. IEEE.
- Liberzon, D. (2003). *Switching in systems and control*, volume 190. Springer.
- Puig, V. (2010). Fault diagnosis and fault tolerant control using set-membership approaches: Application to real case studies.
- Puig, V., Quevedo, J., Escobet, T., and Stancu, A. (2003). Robust fault detection using linear interval observers. *IFAC Proceedings Volumes*, 36(5), 579–584.
- Tang, W., Wang, Z., Zhang, Q., and Shen, Y. (2020). Set-membership estimation for linear time-varying descriptor systems. *Automatica*, 115, 108867.
- Zammali, C., Wang, Z., Van Gorp, J., and Raïssi, T. (2020). Fault detection for switched systems based on pole assignment and zonotopic residual evaluation. *IFAC-PapersOnLine*, 53(2), 4695–4700.
- Zhang, L., Shi, P., Boukas, E.K., and Wang, C. (2007). Robust l2-l filtering for switched linear discrete time-delay systems with polytopic uncertainties. *IET Control Theory & Applications*, 1(3), 722–730.